INTERNATIONAL JOURNAL OF LATEST TECHNOLOGY IN ENGINEERING, MANAGEMENT & APPLIED SCIENCE (IJLTEMAS)
ISSN 2278-2540 | DOI: 10.51583/IJLTEMAS | Volume XV, Issue VII, July 2026

Modifying Operational Efficiency of Static-Structural Loading and Performance Analysis of a Connecting Rod in a Diesel Engine

[1] Atakpa Ojolimi Noah, [2] Inuwa Salamatu [3] *Abioye Mayowa, [4]Jonah Isaac

[1,2]National Space Research and Development Agency, Abuja, Nigeria.

[3]Department of Mechanical Engineering, University of Johannesburg, South Africa.

[4]Department of Mechanical Engineering, Kogi State Polytechnic, Lokoja, Nigeria.

*Correspondence Author

DOI: https://doi.org/10.51583/IJLTEMAS.2026.150700158

Received: 10 August 2026; Accepted: 15 August 2026; Published: 26 August 2026

ABSTRACT

This study presents a finite element analysis-based evaluation of suitable materials for the connecting rod of a diesel engine using ANSYS 2024 R1 simulation. The study focuses on three aluminum-based materials AA356.0-T6, Al7039/Cu/SiC, and Al7050-T7451 to determine their mechanical performance under realistic engine loading conditions. Static structural analysis was conducted to determine the stress distribution, deformation response and elastic strain behaviour of the connecting rod under a peak load of 7.58MPa.

The pressure load of 7.58 MPa was applied at the small end while the big end was fixed. The results revealed that AA356.0-T6 experienced a minimum deformation of 0.24282 mm, von-Mises stress of 124.74 MPa, and equivalent elastic strain of 0.001723. The Al7039/Cu/SiC composite showed a little higher deformation of 0.27311 mm, a corresponding stress of 176.04 MPa and equivalent elastic strain of 0.0017608 whereas Al7050-T7451 demonstrated the highest deformation (0.41653 mm), a high stress of 196.61 MPa and equivalent elastic strain of 0.0023328. The simulation results revealed that AA356.0-T6 exhibited superior stiffness with minimal deformation under static loading.

INTRODUCTION

Connecting rod is one of the important and major components in an internal combustion (IC) engine which provides reciprocating motion from the rotary motion to the crankshaft. In an IC engine the high combustion gas will produce high pressure which lead to high loads development on the connecting rod (Lodhi & Pandey, 2023). Failure of connecting rods is mainly caused by fatigue and factors which results from improper material selection, poor design or fabrication defects (Griza, Bertoni, Zanon, Reguly & Strohaecker, 2009). It is therefore very important to study the behavior of connecting rod in an IC engine for diesel engine due to high pressures on connecting rod. It is also important to study the buckling load of the connecting rod which may reduce the failure of connecting rod. Hence the need for static structural and linear buckling analyses to be conducted on a connecting rod for a diesel engine (Govindraj & Suresha, 2022). Estimation like the maximum stresses, maximum deformation, buckling load factor and critical buckling load are determined for different materials suitable for the manufacturing of connecting rod and this requires some governing laws and theories, such as Rankine in determining the dimensions of the connecting rod (Khurmi & Gupta, 2005).

More efforts have been made to improve the performance of connecting rods. Apart from experimental studies using fracture analysis and microstructural examination, the use of a finite element method (FEM) could aid to improve the design of a connecting rod (Kwaku, Ziblim, Yahaya & Amedorme, 2023).

The finite element method (FEM) is a numerical technique for solving problems which are described by partial differential equations or can be formulated as functional minimization (Manohar & Prashant, 2024). The FEA has been extensively used to solve problems involving complicated and irregular geometries (Manohar & Prashant, 2024). The Commercial software would be employed in this study to divide the solution domain into nodes and elements (ANSYS, 2023). The use of FEM in ANSYS would enhance the identification of the regions of the connecting rod with less von Mises stress to allow for the reduction of weight at the regions (Mohamed et al, 2014) And add weight more to strengthen the region with high von-Mises stress to withstand fatigue failure that normally occurs in the region and as a result increase durability of the connecting rod.

The aim of this study is to carry out the static-structural and performance analysis of a connecting rod in a diesel engine using finite element method in ANSYS. The other specific objectives are:

1. To carry out the design of connecting rod components using relevant equations.

2. To model connecting rod in SOLIDWORKS 2023.

. To import the model into ANSYS 2024R1 commercial software for the static-structural analysis.

. To obtain deformation or deflection, stresses and strains on connecting rod from the static-structural analysis.

. To select the best material for production of the connecting rod based less deformation and superior stiffness that can resist bending or compression more effectively under constant load conditions.

There are many types of connecting rod with different I-section and H-section or X-section which are like a sort of hybrid between I-beam and H-beam and combine the best properties of their predecessors. Connecting rods with an X-beam (Figure 4) are the latest achievement from connecting rod manufacturers. Because of their high rigidity and crack resistance as well as minimal weight, they are basically made for racing.

. Connecting rod without bolt and nut (Figure 1), mostly used in single cylinder engine (Natraj, sandhya, Kumar, Naveen, Vivek, 2022)

. Connecting rod with bolt and nut (Figures 2, 3 & 4); the connecting rod with cap at the big end is joined by means of bolt and nut. This type of connecting rod is most widely used in multi cylinder engines.

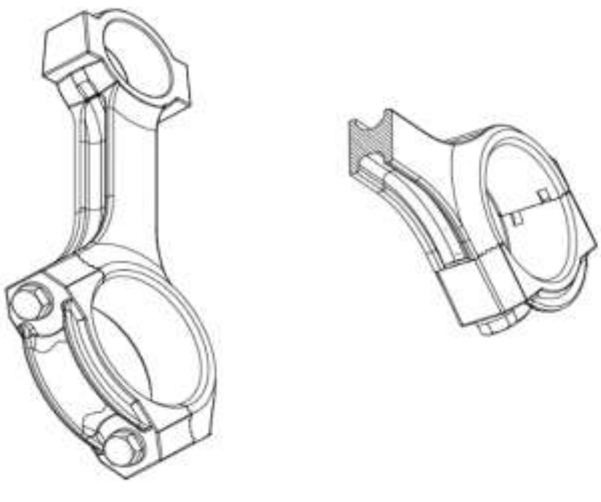

Figure 1 Connecting Rod without Bolt

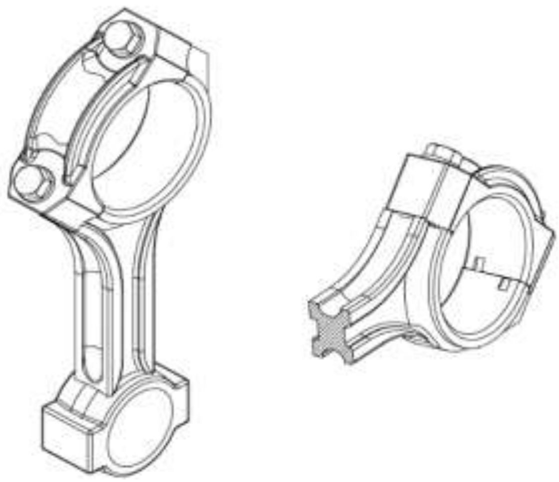

Figure 2: I-Beam Connecting Rod

ISSN 2278-2540 | DOI: 10.51583/IJLTEMAS | Volume XV, Issue VII, July 2026

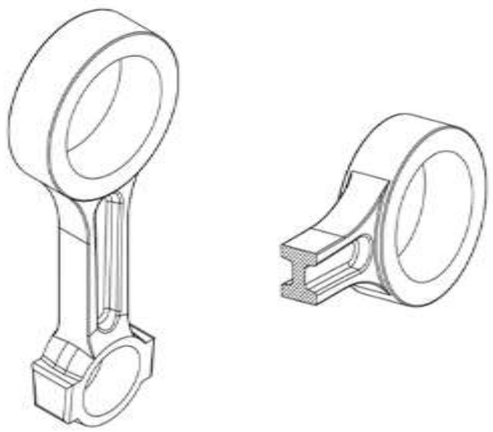

Figure 3 H-Beam Connecting Rod

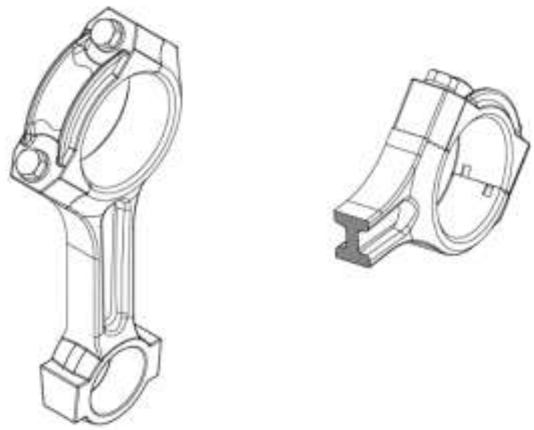

Figure 4 X-beam, Cross Beam

MATERIALS AND METHODS

The research utilizes the material for this study are AA356.0-T6, Al7050-T7451 and Aluminum Metal Matrix Composites Al7039/Cu/SiC for its better thermal conductivity than aluminum alloys.

Tables 1 shows the Chemical composition of the connecting rod materials while Table 2 shows the Mechanical, Physical and Thermal properties of the selected materials for the connecting rod.

H-Beam (Figure 3) can take care of large stress and anxiety without flexing so used in high power engines. I - beam (Figure 2) manage high-pressure, light and strong. In a study H-beam profile is better than I-beam profile because it has more stability – up to 43.1% and von Mises stresses are also less up to 12.3% (average – 15.7%). But I-beam is being used more as it is easier and less expensive to manufacture it (Godara, Brenia, Soni, Shekhawat, & Saxena, 2022); hence I-beam is used for this study.

Table 1Chemical composition of the connecting rod materials

Element	AA 356.0-T6	Al7050-T7451	Al 7039/Cu/SiC
Iron, Fe (%)	0.6	0.15	0.35
Chromium (%)		0.04	0.1
Manganese, Mn (%)	0.35	0.1	0.03
Zinc, Zn (%)	0.35	5.7 – 6.7	0.05
Silicon, Si (%)	7.5	0.12	0.84
Silicon Carbide (%)			15
Al	90.1	87.3 – 90.3	69.22
Titanium, Ti	0.25	0.06	0.03
Zr		0.08 – 0.15	
Magnesium, Mg	0.45	1.9 – 2.6	0.02
Copper, Cu	0.25	2 – 2.6	12
Others	0.15	0.15	

Table 2Mechanical, Physical and Thermal properties of the connecting rod material

ISSN 2278-2540 | DOI: 10.51583/IJLTEMAS | Volume XV, Issue VII, July 2026

Element	AA 356.0-T6	Al7050-T7451	Al 7039/Cu/SiC
Tensile strength (MPa)	131MPa	524MPa	610MPA
Compressive Yield strength	90MPa	434MPa	400MPa
Shear modulus (typical for steel)	27.2GPa	26.9GPa	26.9GPa
Elastic modulus	72.4GPa	72GPa	100GPa
Poisson's ratio	0.33	0.33	0.30
Density(g/cm^3)	2.6	2.83	2.73
Thermal expansion co-efficient (µm/m°C)	21.4	23.6	18.55
Thermal conductivity (typical steel) (W/Mk)	150	157	169.6
Specific Heat(J/kg.K)	963	860	745.8

The Design Input parameters were obtained from the WP10.336 Weichai diesel engine.

Weichai Diesel Engine consists of six cylinders pistons. The details are as tabulated below (Weichai Power Company Limited, 2017), https://en.weichai.com/

Table 3 Engine specifications for WP10.33 diesel engine

SN	Parameter	Symbol	Value	Unit
1	Engine Model	WP10.336		
2	Engine Type	Turbocharged-Intercool	6	Cylinders
3	Engine Capacity	V_s	9726	ml
4	Bore Diameter	d	126	mm
5	Stroke	s	130	mm
6	Con Rod Length	l	219	mm
7	Rated Speed	N	1900	rpm
8	Rated Power		247	Kw
9	Mass of connecting rod	Mc	3.708	Kg
10	Mass of Piston Assy & Pin	Mp	7.188	Kg
11	Max Combustion Temperature		1001	K
12	Max Combustion Pressure	Pg	7.58	N/mm^2
13	Max torque		1500	Nm

METHOD

The methods applied in this study were as follows:

. Designing of connecting rod components (piston pin, shank with big and small ends, cap for crank end and bolts for the cap) using relevant equations.

ISSN 2278-2540 | DOI: 10.51583/IJLTEMAS | Volume XV, Issue VII, July 2026

2.Modeling of the designed connecting rod in SOLIDWORKS

. Importation of the model into ANSYS commercial software for simulation

. Meshing of the model with 3mm mesh size

. Carrying out the static-structural and performance analysis to obtain the stresses and strains by considering material variations of the model to reduce deformation and von-Mises and strain.

6.Analyze the various results obtain from the selected materials

7.Zero-in on the most efficient material during static-structural analysis

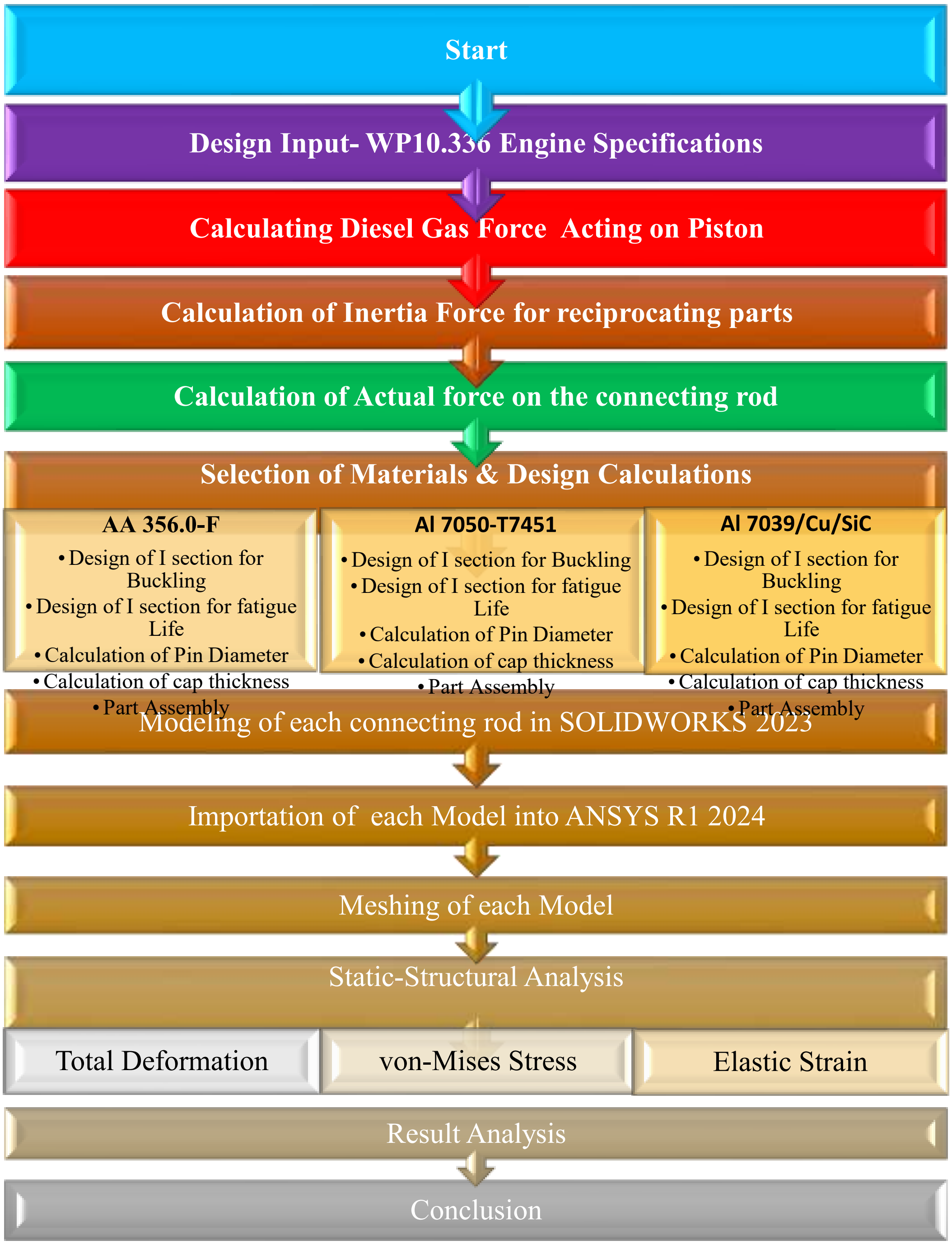

Flow Chart

ISSN 2278-2540 | DOI: 10.51583/IJLTEMAS | Volume XV, Issue VII, July 2026

Design Calculations of Connecting Rods using the Selected Materials

Pressure for WEICHAI WP10.336 Diesel Engine

n = 6; Max. Speed = 1900rpm, Maximum combustion pressure =7.58MPa, Combustion Gas Temperature 1001K from weichai engine data

All equations were obtained from Khurmi, R. and Gupta, J.K., (2005) A Textbook of Machine Design Text of Machine Design. Eurasia Publishing House (Pvt.) Ltd., New Delhi.]

Calculation of Force due Gas Pressure

$$F_p = P * A = 7.58 * \frac{\pi D^2}{4} = 7.58 * \frac{\pi (126)^2}{4} = 94527.1328N$$

Calculation of force due to Inertia

$$Inertia\ Force, F_I = m \cdot \omega^2 \cdot r \left(cos\,\theta + \frac{cos\,2\theta}{n} \right)$$

$$n = \frac{l}{r} = \frac{2 \times stroke}{stroke/_2} = 4$$

The maximum gas load occurs shortly after the dead centre position at θ = 3.3°, Cos3.3 = 0.9983≅ 1

$$F_I = 1.394 \times \left(\frac{2\pi \times 1900}{60} \right)^2 \times 0.065 \times \left(1 + \frac{1}{4}\right) = 4483.8449$$

Total Force acting $F = F_p \pm F_I$

Where,

F_P = force acting on the piston

F_I = force of inertia

$$F = 94527.1328N - 4483.8449 = 90043.28794N$$

Now let us find the dimensions of this I-section. Since the connecting rod is designed by taking the force on the connecting rod (F_P) equal to the maximum force on the piston (F_L) due to gas pressure, therefore,

We know that the connecting rod is designed for buckling about X-axis (i.e. in the plane of motion of the connecting rod) assuming both ends hinged. Taking 2 as presume safety factor, therefore the buckling load,

$$W_{\boldsymbol{B}} = F \times 2 = 180086.27588$$

$$W_B = \frac{\sigma_c\ .\ A}{1 + a\left(\frac{L}{K_{xx}}\right)^2}$$

$$A = 2\,(4\,t \times t) + 3\,t \times t = 11\,t^2$$

Moment of inertia of the section about X-axis: I_{xx}

ISSN 2278-2540 | DOI: 10.51583/IJLTEMAS | Volume XV, Issue VII, July 2026

$$I_{xx} = \frac{1}{12}[4t \times (5t)^3 - 3t(3t)^3] = \frac{419}{12}t^4$$

Moment of inertia of the section about Y-axis: I_{yy}

$$I_{yy} = \left[2 \times \frac{1}{12}t \times (4t)^3 + \frac{1}{12}(3t)t^3\right] = \frac{131}{12}t^4$$

$$\frac{I_{xx}}{I_{yy}} = \frac{419}{12} \times \frac{12}{131} = 3.2$$

Since the ratio of the moment of inertia of I_{xx} *to* I_{yy} *is* 3.2 *the* design shape satisfied the buckling condition.

Calculation of the radius of gyration

The radius of gyration about X- axis is

Substitute for the values in equation 2.19

$$\mathrm{K_{xx}} = \sqrt{\frac{\mathrm{I_{xx}}}{\mathrm{A}}} = \sqrt{\frac{419}{12}\mathrm{t}^4 \times \frac{1}{11\,\mathrm{t}^2}} = 1.7816\mathrm{t}$$

Design Calculation for the Connecting Rod using AA 356.0-T6 Aluminum Alloy

$$\sigma_c = 90\mathrm{MPa};\ \ a = \frac{1}{9000};\ L = l = 219\mathrm{mm}, \text{ie connecting } \textit{rod hinged} \text{ at both ends} = 219\mathrm{mm} \text{ from engine manual}$$

Thickness of the I-section web, t

$$180086.27588 = \frac{90 \times 10^6 \times 11\,\mathrm{t}^2}{1 + \frac{1}{9000} \times \left(\frac{0.219}{1.7816\mathrm{t}}\right)^2} = \frac{99 \times 10^7\,\mathrm{t}^4}{\mathrm{t}^2 + 1.678902 \times 10^{-6}}$$

$$180086.27588\,(\mathrm{t}^2 + 1.678902 \times 10^{-6}) = 99 \times 10^7 \times \mathrm{t}^4$$

$$180086.27588\,\mathrm{t}^2 + 0.3023477 = 99 \times 10^7\,\mathrm{t}^4$$

$$-99 \times 10^7\mathrm{t}^4 + 180086.27588\,\mathrm{t}^2 + 0.33244 = 0$$

$$\mathrm{t} = -0.013417 \times 10^7\mathrm{m};\ 0.013417 \times 10^7\mathrm{m}; (1.365696 \times 10^7\mathrm{m})\mathrm{i}; (-1.36569 \times 10^7\mathrm{m})\mathrm{i}$$

The solution gave two real roots and two complex roots, hence the selection of positive real root

$$\therefore \mathrm{t} = 13.417\mathrm{mm} \cong 13\mathrm{mm}$$

$$\mathrm{H} = 5\mathrm{t} = 5 \times 13 = 65\mathrm{mm}$$

$$\mathrm{B} = 4\mathrm{t} = 4 \times 13 = 52\mathrm{mm}$$

$$\mathrm{H_1} = 1.25 * \mathrm{H} = 1.25 * 65 = 81.25 \cong 81\mathrm{mm}$$

$$\mathrm{H_2} = 0.9 * \mathrm{H} = 0.9 * 65 = 58.5 \cong 59\mathrm{mm}$$

The above calculations were applied to each of the materials and below are the designed dimensions

ISSN 2278-2540 | DOI: 10.51583/IJLTEMAS | Volume XV, Issue VII, July 2026

Table 5: Dimensions of designed connecting rod for the selected materials

Items Descriptions	Connecting rod Dimensions for selected Materials(mm)		
	AA 356.0-F	Al7050-T7451	Al 7039/Cu/SiC
Thickness of connecting rod (t)	13	6	7
Height of the section (H)	65	30	35
Width of the section (B)	52	24	28
Height at the Big End (H1)	81	38	44
Height at the small end (H2)	59	27	32
Inner diameter of the Small End(dp)	60	60	60
Outer diameter of the Small End(Dp)	86	86	86
Inner diameter of the Big End (dc)	88	88	88
Outer diameter of the Big End(Dc)	132	120	120
Thickness of the big end cap (t_c)	29	13	13

RESULTS AND DISCUSSIONS

This section presents and discusses the results of the ANSYS 2024 R1simulations carried out to evaluate the performance of three different materials AA356.0-T6, Al7039/Cu/SiC, and Al7050-T7451 used for the connecting rod of a diesel engine. Static-structural analysis was conducted during the simulations. The analysis provided critical insights into the mechanical response of the selected materials under realistic operating conditions. These findings form the basis for selecting the most suitable material for optimal connecting rod performance (Kumar et al., 2021; Rajasekaran et al., 2022).

Static Structural Analysis using ANSYS 2024R1

AA365.0-T6 Static Structural Analysis

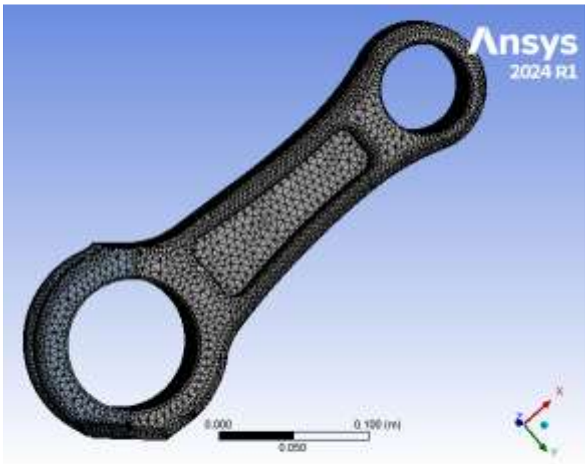

Figure 5 AA356.0-F Mesh

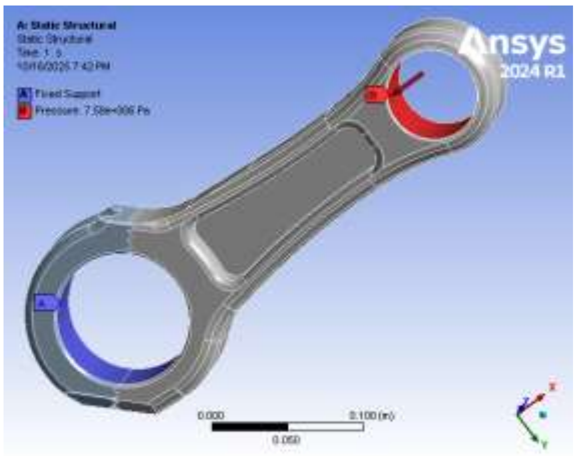

Figure 6 Boundary conditions

Mesh into 108058 nodes and 61236 elements tetrahedron element type and element size of 3mm.

ISSN 2278-2540 | DOI: 10.51583/IJLTEMAS | Volume XV, Issue VII, July 2026

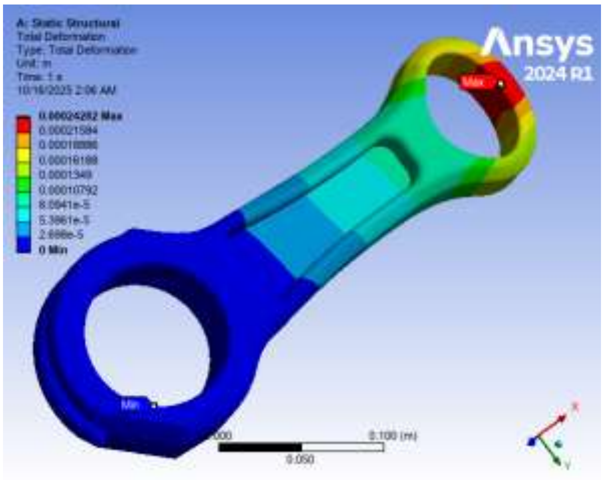

Figure 7 Total Deformation

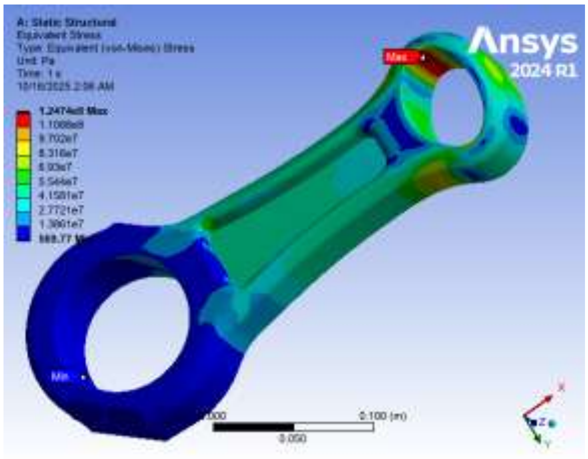

Figure 8 Von Mises Stress

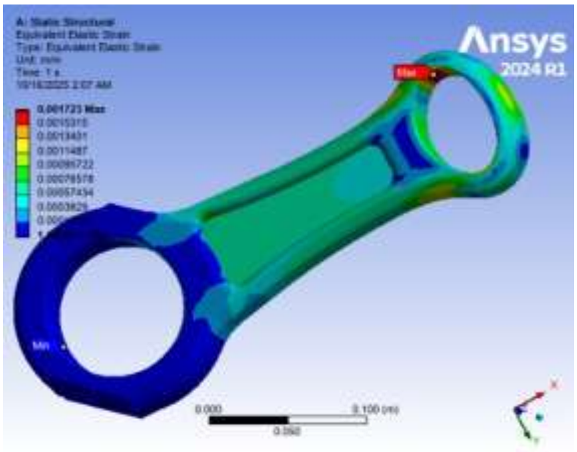

Figure 9 Equivalent Elastic Strain

Al7039/Cu/SiC Static Structural Analysis

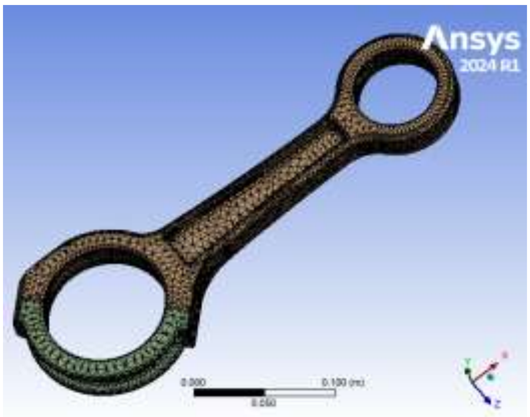

Figure 10 Mesh

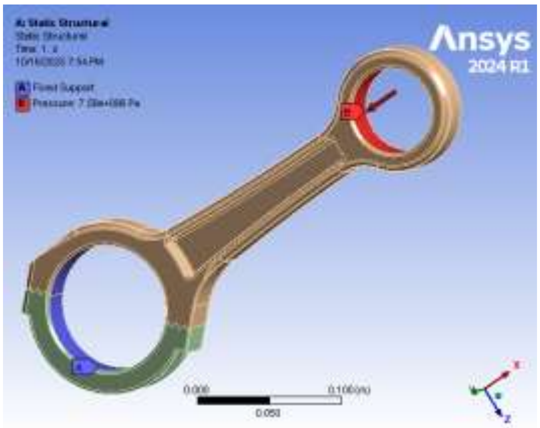

Figure 11 Boundary Conditions

Mesh into 80297 nodes and 45262 elements tetrahedron element type and element size of 3mm.

ISSN 2278-2540 | DOI: 10.51583/IJLTEMAS | Volume XV, Issue VII, July 2026

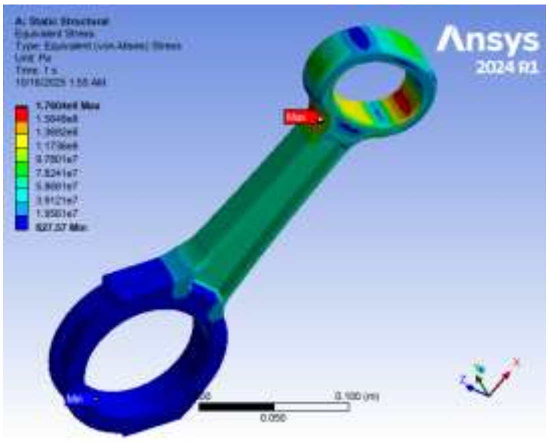

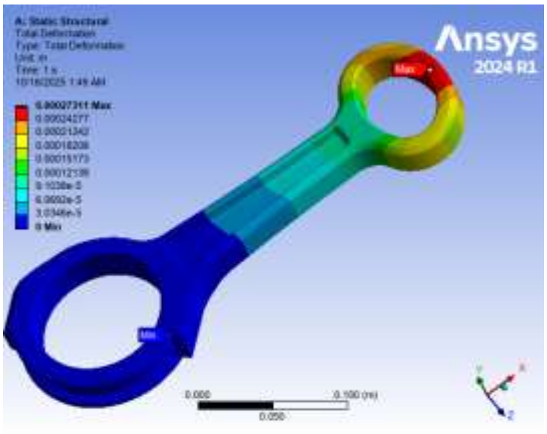

Figure 12 Total Deformation **Figure 13** Von Mises Stress

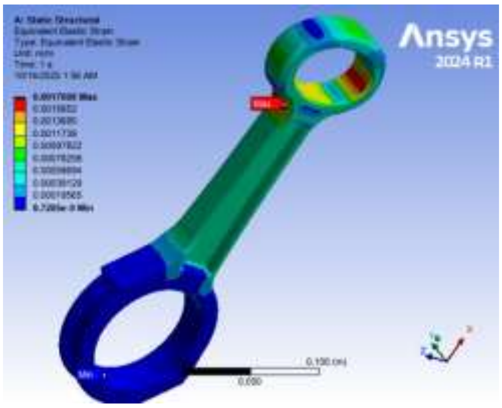

Figure 14 Equivalent Elastic Strain

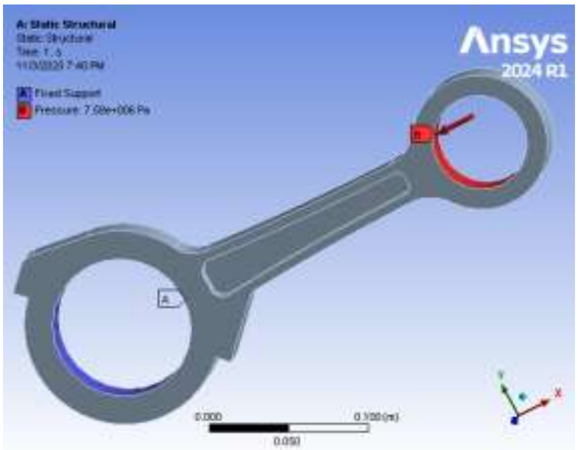

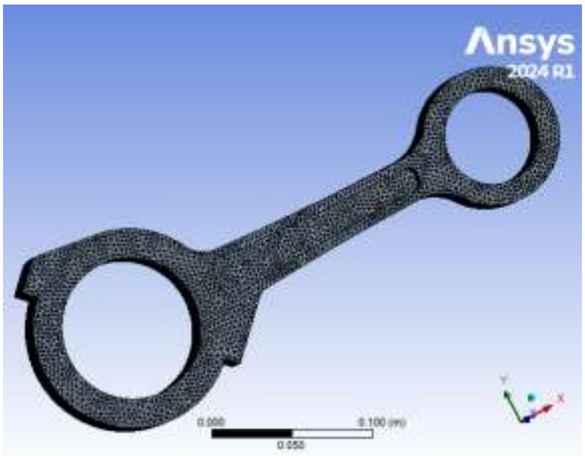

Al7050-T7451 Static Structural Analysis

Figure 15 Mesh **Figure 16** Boundary Condition

Tetrahedron mesh with element size of 3mm to get 221910 nodes and 151261 elements.

ISSN 2278-2540 | DOI: 10.51583/IJLTEMAS | Volume XV, Issue VII, July 2026

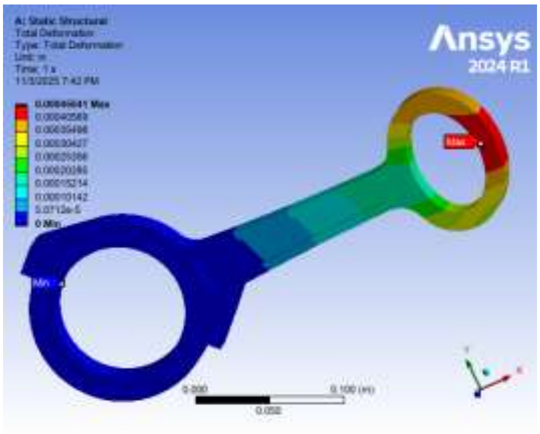

Figure 17 Total Deformation

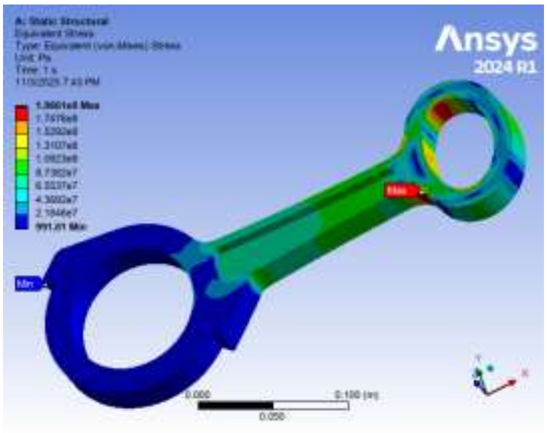

Figure 18 Von Mises Stress

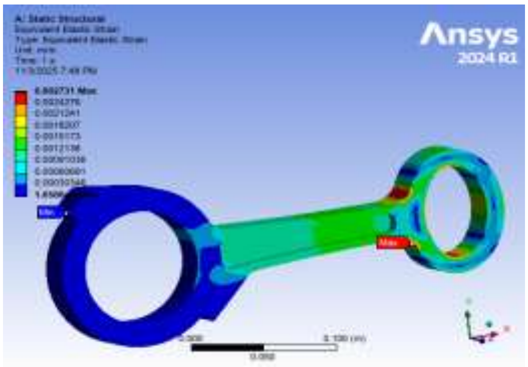

Figure 19 Equivalent Elastic Strain

Table 6 Results of Static Structural Analysis (Figures 5 – 19)

Model		Total Deformation(mm)	Von-Mises Stress (MPa)	Equivalent Elastic Strain(m/m)
AA35A356.0-T6	Max	0.24282	124.74	0.001723
	Min	0	0.0005.6978	$1.1828x10^{-8}$
Al7039/Cu/SiC	Max	0.27311	176.04	0.0017608
	Min	0	0.00082757	$8.7205x10^{-9}$
AlA7050-T7451	Max	0.41653	167.96	0.0023328
	Min	0	0.00038425	$9.6012x10^{-9}$

ISSN 2278-2540 | DOI: 10.51583/IJLTEMAS | Volume XV, Issue VII, July 2026

Graphical Representation of Static Structural Analysis

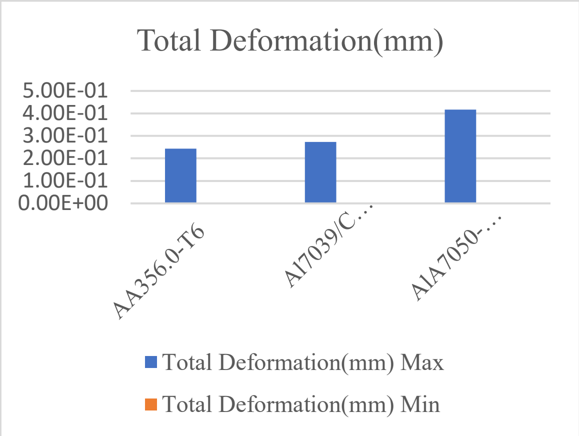

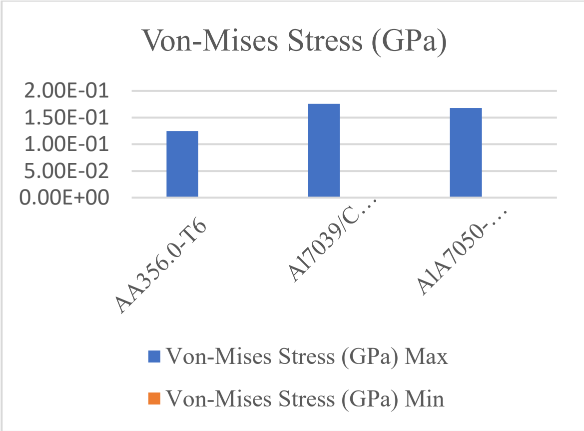

Figure 20 Total Deformation Comparison **Figure 21** Von-Mises Stress Comparison

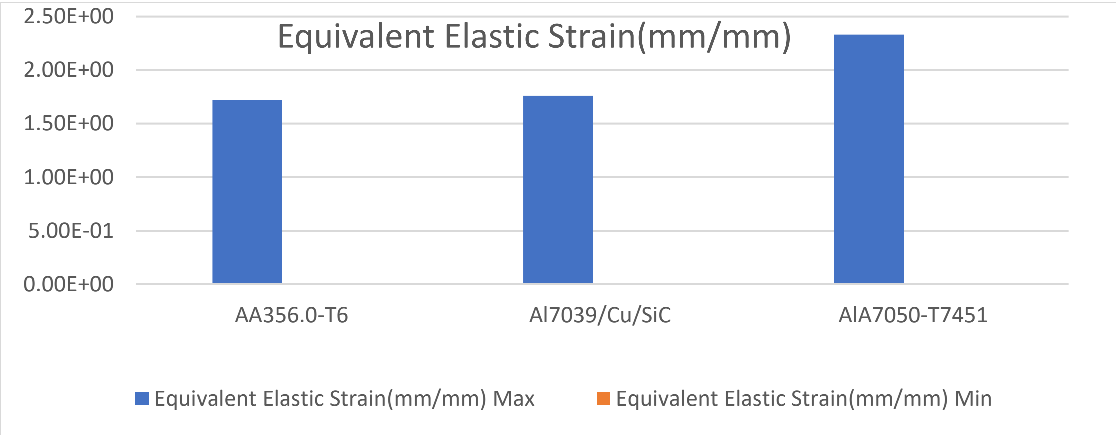

Figure 22 Equivalent Elastic Strain Comparative Chart

Discussion and Interpretation of Results on Static Structural Analysis

The static structural analysis determined how each material deforms and withstands stress under load. The results, shown in Figures 5- 19 with graphical representations (figures 20 – 22), indicate that AA356.0-T6 exhibited the lowest total deformation and stress concentration, followed by Al7050-T7451, while Al7039/Cu/SiC displayed slightly higher stress magnitudes. This suggests that AA356.0-T6 possesses superior stiffness and can resist bending or compression more effectively under constant load conditions (Sharma & Chauhan, 2020). It is dimensional stable. This behavior suggests that AA356.0-T6 possesses a higher modulus of elasticity and enhanced resistance to plastic deformation, which are essential attributes for structural applications requiring minimal deflection under load (Azadi, Hashemi, & Nili-Ahmadadi, 2013; Teng, Lu, & Chen,2023)

In contrast, Al7039/Cu/SiC demonstrates the highest equivalent elastic strain (figure 22) and slightly elevated Von-Mises stress values (figure 21), implying that this hybrid composite can withstand greater elastic deformation while maintaining comparable strength. Such characteristics are advantageous in applications subjected to fluctuating or impact loads, where controlled flexibility and stress redistribution are desirable (Avci, Turan, & Guler, 2017; Teferi, 2025; Adebayo & Oyetunji, 2025).

In summary, AA356.0-T6 demonstrates the most favorable balance of stiffness and toughness, Al7039/Cu/SiC offers superior elastic flexibility and strength retention, and AlA7050-T7451 provides moderate mechanical properties with limited uniformity. These distinctions underscore the necessity of aligning material selection with specific mechanical and operational requirements.

ISSN 2278-2540 | DOI: 10.51583/IJLTEMAS | Volume XV, Issue VII, July 2026

Applications and future recommendations

For a more advanced study, Design of Experiments (DOE) can be used to systematically investigate the effects of different geometric parameters on connecting-rod performance. Rather than changing one parameter at a time, DOE allows multiple design variables to be studied systematically.

For example, the following variables can be investigated:

- Shank thickness;
- Shank width;
- Web thickness;
- Fillet radius;
- Small-end thickness;
- Big-end thickness.

The corresponding responses may include:

- Mass;
- Maximum von Mises stress;
- Total deformation;
- Factor of safety;
- Maximum strain;
- Buckling load factor.

Statistical techniques such as Analysis of Variance (ANOVA) can subsequently be used to determine which geometric parameters have the greatest influence on the structural performance of the connecting rod. This approach can complement FEA-based optimization by providing quantitative evidence of the relative influence of the selected design variables.

Engineering Benefits

A successful optimized connecting-rod design can provide several engineering benefits. First, reducing the reciprocating mass can reduce inertia effects within the engine. Second, a structurally efficient connecting rod may reduce material requirements and manufacturing costs. Third, optimization can improve the strength-to-weight ratio of the component. Fourth, improved stress distribution can reduce the likelihood of premature failure around critical regions (Shenoy & Fatemi, 2005; Murthy et al., 2019).

The optimization process can also contribute to improved engine reliability by reducing stress concentrations and ensuring that the connecting rod has sufficient structural capacity under critical operating conditions. Furthermore, the application of FEA and numerical optimization can reduce the need for repeated physical prototypes, thereby lowering development costs and shortening the design-development cycle.

CONCLUSION

Overall, the comparative assessment highlights the importance of tailored material selection in advanced engineering applications. By correlating mechanical responses with design requirements, engineers can optimize

ISSN 2278-2540 | DOI: 10.51583/IJLTEMAS | Volume XV, Issue VII, July 2026

both performance and safety margins, ensuring that each alloy is utilized to its full structural potential. From an application standpoint, the findings emphasize that AA356.0-T6 is the most suitable material for high-rigidity structural components, such as automotive chassis members, aerospace framework, and precision cast structural parts, where dimensional stability and resistance to deformation are paramount (Azadi et al., 2013; Teng et al., 2023).

REFERENCES

1. Adebayo, K. O., & Oyetunji, A. (2025). Effect of compositions weight fraction on surface roughness of Al7039/Cu/SiC MMCs: A central composite design approach. Bohrium Engineering Journal, 7(2), 115–123. https://www.bohrium.com/paper-details/effect-of-compositions-weight-fraction-on-surface-roughness-of-al7039-cu-sic-mmcs-a-central-composite-design-approach
2. ANSYS (2023). ANSYS Topology Optimization User's Guide. ANSYS, Inc
3. Autodoc blog expert in auto parts-(online) 2023, Engine connecting rod: functions, problems, and failure symptoms
4. Avci, U., Turan, M. E., & Guler, S. (2017). A new approach to the production of partially graded and SiC-reinforced Al7039 alloy matrix composites. Composites Part B: Engineering, 131, 216–225. https://doi.org/10.1016/j.compositesb.2017.08.041
5. Azadi, M., Hashemi, R., & Nili-Ahmadabadi, M. (2013). Heat treatment effect on thermo-mechanical fatigue and low-cycle fatigue behaviours of A356.0 and A356.0-T6 aluminium alloys. Materials Science and Engineering: A, 559, 161–168. https://doi.org/10.1016/j.msea.2012.08.045
6. Godara,S.S, BreniaV., Soni A. K., Shekhawat R. S., & Saxena K.K., (2022), Design & analysis of connecting rod using ANSYS software, Materialstoday Proceedings, Volume 56, Part 4, April 2022, Pages 1896-1903, https://doi.org/10.1016/j.matpr.2021.11.166
7. Govindraj N, S. Suresha, (2022), Static structural and linear buckling analysis of diesel generator connecting rod
8. Griza S, Bertoni F., Zanon G., Reguly A., Strohaecker T.R (2009) Fatigue in engine connecting rod bolt due to forming laps Eng. Fail. Anal., (2009).
9. Khurmi, R. and Gupta, J.K., (2005) A Textbook of Machine Design Text of Machine Design. Eurasia Publishing House (Pvt.) Ltd., New Delhi.]
10. Kumar S.,VermaV., Gupta N,(2021) Design and FEM Analysis of Connecting Rod of different Materials, Lecture note in Mechanical Engineering, Springer Singapore
11. Kwaku N. J., Ziblim B., Yahaya S., Amedorme S. K., (2023), Modal and Thermal Analysis of a Modified Connecting Rod of an Internal Combustion Engine Using Finite Element Method, Modeling and Numerical Simulation of Material Science, 13, 29-49
12. Lodhi A. K, Prof. Pandey P, K, (2023), A Review on Design Optimisation of Connecting Rod, International Journal of Scientific Research & Engineering Trends Volume 9, Issue 1, Jan-Feb-2023
13. Manohar G., Prof. Prashant K., (2024), Optimization and Analysis of 4-Wheeler Connecting Rod for Weight Reduction and Performance Enhancement
14. Mohamed H. A., Sinha E. P. K., Dr. Darbari A. S., (2014) Design and Analysis of Connecting Rod using Aluminium Alloy 7068 T6, T6511 IJMET (2014), International Journal of Mechanical Engineering and Technology, Volume 5, Issue 10, October (2014), pp. 57-69.
15. Nkrumah J., K, Ziblim B., Yahaya S., Amedorme S. K., (2023), Modal and Thermal Analysis of a Modified Connecting Rod of an Internal Combustion Engine Using Finite Element Method, Modeling and Numerical Simulation of Material Science, **13**, 29-49
16. Shenoy, P. S., & Fatemi, A. (2005). Connecting rod optimization for weight and cost reduction. SAE Technical Paper 2005-01-0987. SAE International. https://doi.org/10.4271/2005-01-0987
17. Teferi, F. T. (2025). Elevating Al7039 alloy performance through copper addition. Materials Research Express, 12(1), 016502. https://doi.org/10.1088/2053-1591/ada672
18. Teferi, F. T., Kolhe K. P., Tsegaw A. A., & Fatoba S. O.(2025) Optimization of SiC reinforced Al7039/Cu composites for enhanced thermal conductivity and hardness via response surface methodology, Published 8 January 2025 • © 2025 The Author(s). Published by IOP Publishing Ltd, Materials Research Express, Volume 12, Number 1, https://doi.org/10.1088/2053-1591/ada2e3

ISSN 2278-2540 | DOI: 10.51583/IJLTEMAS | Volume XV, Issue VII, July 2026

19. Teng, D., Lu, P., & Chen, Y. (2023). Response of mechanical properties of A356 alloy to different processing parameters. Materials Research Express, 10(5), 055004. https://doi.org/10.1088/2053-1591/acd250
20. Weichai Power Company Limited (2017), Operation and Maintenance Manual forWP10 Series Four-valve Diesel Engine (China IV, V), June 2017